Journal of Materials Chemistry B

Accepted Manuscript

ROYAL SOCIETY OF CHEMISTRY

www.rsc.org/materialsB

Journal of Materials Chemistry B

Cite this: DOI: 10.1039/c0xx00000x

PAPER

www.rsc.org/xxxxxx

Formation of iron oxide nanoparticle-loaded γ-polyglutamic acid nanogels for MR imaging of tumors†

Jianzhi Zhu,[a1] Chen Peng,[b1] Wenjie Sun,[a] Zhibo Yu,[c] Benqing Zhou,[a] Du Li,[c] Yu Luo,[a] Ling Ding,[a] Mingwu Shen,[a] and Xiangyang Shi[a,c]*

Received (in XXX, XXX) Xth XXXXXXXXX 20XX, Accepted Xth XXXXXXXXX 20XX
DOI: 10.1039/b000000x

We report a facile approach to forming iron oxide nanoparticle (NP)-loaded γ-polyglutamic acid (γ-PGA) nanogels for MR imaging of tumors. In this study, γ-PGA with carboxyl groups activated by 1-ethyl-3-[3-dimethylaminopropyl] carbodiimide hydrochloride (EDC) in aqueous solution was firstly emulsified, followed by *in situ* chemical crosslinking with polyethyleneimine (PEI)-coated iron oxide NPs (PEI-Fe_3O_4 NPs) with a core size of 8.9 ± 2.1 nm synthesized *via* a mild reduction route. The formed γ-PGA nanogels containing iron oxide NPs (γ-PGA/PEI-Fe_3O_4 NGs) with a size of 152.3 ± 13.1 nm are water-dispersible, colloidally stable, noncytotoxic in a given concentration range, and display a r_2 relaxivity of 171.1 $mM^{-1}s^{-1}$. Likewise, the hybrid nanogels can be uptaken by cancer cells with an Fe uptake significantly higher than single Fe_3O_4 NPs. These properties render the formed γ-PGA/PEI-Fe_3O_4 nanogels with an ability to be used as an effective contrast agent for MR imaging of cancer cells *in vitro* and the xenografted tumor model *in vivo via* the passive enhanced permeability and retention effect after intravenous injection. The developed γ-PGA/PEI-Fe_3O_4 hybrid nanogels may hold great promise to be used as a novel contrast agent for MR imaging or other theranostic applications.

Introduction

As a powerful noninvasive imaging modality, magnetic resonance (MR) imaging has attracted substantial attention in the early detection and diagnosis of cancer or other diseases due to its high spatial resolution, superior soft tissue contrast, multi-dimensional imaging, and lack of radiological consequences.[1-4] To further improve the imaging quality and sensitivity, a wide variety of MR contrast agents, such as superparamagnetic iron oxide nanoparticles (Fe_3O_4 NPs),[5-7] manganese oxide NPs[8] and gadolinium chelates[9] have been developed. In particular, superparamagnetic Fe_3O_4 NPs have been used as T_2-weighted MR contrast agents.[3, 4, 10-12] For improved MR imaging quality, Fe_3O_4 NPs have to be functionalized to have desirable colloidal stability, and targeting specificity in order to have specific and enhanced uptake in a specific type of cells.

In our previous work, we reported a facile hydrothermal synthesis approach to generating Fe_3O_4 NPs coated with branched polyethyleneimine (PEI) with good colloidal stability and a relatively high r_2 relaxivity.[13] The formed PEI-coated Fe_3O_4 NPs can be further modified with targeting ligands such as hyaluronic acid[4] or folic acid (FA)[6] for targeted MR imaging of CD44 receptor- or FA receptor-overexpressing tumors. Similarly, the PEI-coating approach can be extended to prepare stable Fe_3O_4 NPs with ultrahigh r_2 relaxivity for sensitive and specific imaging of other types of tumors.[14, 15] Besides the single particle surface modification approach, Fe_3O_4 NPs can also be modified to form a type of assembly or a clustered structure in order to have improved cellular uptake or r_2 relaxivity. For instance, a recent report by Ai *et al.* has shown that hydrophobic superparamagnetic Fe_3O_4 NPs or manganese ferrite NPs can be incorporated within micelles formed using an amphiphilic diblock copolymer poly-(ε-capro-lactone)-*b*-poly(ethyelene glycol).[16, 17] The formed polymer micelles loaded with Fe_3O_4 NPs displayed dramatically increased r_2 relaxivity when compared to the single Fe_3O_4 NPs, which is beneficial for sensitive MR imaging applications. The enhanced r_2 relaxivity is presumably due to the fact that clustered Fe_3O_4 NPs may have enhanced local accessibility of water protons or display enhanced magnetic dipole interactions. Therefore it is reasonable to incorporate Fe_3O_4 NPs within a micro or nanocompartment aiming to improve their MR imaging performances.

Polymer nanogels (NGs) have recently gained extensive interest in the field of drug and gene delivery,[18] likely due to their inheritance of the superiority of bulk hydrogels as well as characteristics of NPs. Due to the softness and excellent fluidity, NGs can be easily endocytosed by different types of cells, thereby having enhanced drug/gene delivery and biomedical imaging applications.[19-25] For instance, Nochi *et al.* reported the development of pullulan NGs as an intranasal vaccine delivery system, which significantly enhanced vaccine-induced systemic and mucosal antibody production.[26] As a kind of naturally occurring biodegradable polymer synthesized by microbial

species, γ-polyglutamic acid (γ-PGA) has been widely adopted for oral drug delivery,[27] wound dressing and tissue engineering.[28-31] Inspired by the advantages of NGs with enhanced cellular uptake and the possible improvement of the r_2 relaxivity of the Fe_3O_4 NPs caused by the clustering effects in a microenvironment, the aim of this work is to develop a rather new approach to preparing Fe_3O_4 NP-loaded γ-PGA NGs for MR imaging applications.

In this present study, we developed a double emulsion approach to forming Fe_3O_4 NP-loaded γ-PGA NGs for T_2-weighted MR imaging of tumors. γ-PGA with carboxyl groups activated by 1-ethyl-3-[3-dimethylaminopropyl] carbodiimide hydrochloride (EDC) in aqueous solution was firstly emulsified, followed by *in situ* chemical crosslinking with PEI-coated Fe_3O_4 NPs (PEI-Fe_3O_4 NPs) synthesized *via* a mild reduction route. The formed γ-PGA/PEI-Fe_3O_4 NGs were well characterized. Their cytotoxicity was assessed *via* quantitative cell viability assay and cell morphology observation. The cellular uptake of the NGs was evaluated by qualitative Prussian blue staining and quantitative inductively coupled plasma-optical emission spectroscopy (ICP-OES) measurements. Lastly, the γ-PGA/PEI-Fe_3O_4 NGs were used as a contrast agent for MR imaging of cancer cells *in vitro* and the xenografted tumor model *in vivo*. To our knowledge, this is the first report related to the generation of Fe_3O_4 NP-loaded γ-PGA NGs for MR imaging applications.

Experimental

Materials

Materials: γ-PGA (Mw = 1000 kDa) was acquired from Nanjing Saitesi Co., Ltd (Nanjing, China). 1-Ethyl-3-[3-dimethylaminopropyl] carbodiimide hydrochloride (EDC) was purchased from J&K Chemical Ltd (Shanghai, China). Ferric chloride hexahydrate ($FeCl_3 \cdot 6H_2O$ > 99%), dioctyl sodium sulfosuccinate (AOT), sodium sulfite (Na_2SO_3), and sodium bicarbonate ($NaHCO_3$) were obtained from Sinopharm Chemical Reagent Co., Ltd (Beijing, China). Dichloromethane (DCM), ammonia ($NH_3 \cdot H_2O$, 25-28% NH_3 in water solution) and succinic anhydride were purchased from Shanghai Lingfeng Chemical Reagent Co., Ltd. (Shanghai, China). Poly(vinyl alchol) (PVA, 88% hydrolyzed, Mw = 20 - 30 kDa) was purchased from Acros Oganics (Geel, Belgium). L-Glutathione (GSH) was obtained from Biosharp Co., Ltd. (Hefei, China). Cell Counting Kit (CCK-8) was purchased from 7Sea Pharmatech Co., Ltd. (Shanghai, China). Branched PEI (Mw = 25 kDa) and all the other chemicals and solvents were supplied by Aldrich (St. Louis, MO). HeLa cells (a human cervical carcinoma cell line) were obtained from Institute of Biochemistry and Cell Biology, the Chinese Academy of Sciences (Shanghai, China). Fetal bovine serum (FBS), Dulbecco's modified Eagle's medium (DMEM), penicillin, and streptomycin were obtained from Hangzhou Jinuo Biomedical Technology (Hangzhou, China). Water used in all experiments was purified by a Milli-Q Plus 185 water purification system with a resistivity higher than 18.2 MΩ·cm (Millipore, Bedford, MA).

Formation of γ-PGA/PEI-Fe_3O_4 NGs

PEI-Fe_3O_4 NPs and naked Fe_3O_4 NPs were prepared by a mild reduction route according to protocols reported in the literature.[14] Using the PEI-Fe_3O_4 NPs as a crosslinker, γ-PGA/PEI-Fe_3O_4 NGs were formed *via* a double emulsion method as described in the literature.[32, 33] Briefly, γ-PGA (20 mg) dissolved in 2 mL water was activated by EDC (30 mg) under stirring for 2 h at room temperature, followed by addition of $NaHCO_3$ (26 mg) to decrease the electrostatic interaction between the PEI amines and the γ-PGA carboxyl groups. Then the mixture was dropwise added into a DCM solution (4 mL) containing AOT (134 mg) under stirring for 10 min to form a water-in-oil (W/O) emulsion. Thereafter, the above dispersion was dropwise added into an aqueous PVA solution (600 mg PVA, 30 mL) under stirring for 15 min to form a W/O/W emulsion. Finally, the PEI-Fe_3O_4 NPs (33.36 mg) dispersed in 5 mL water were dropped into the above dispersion under stirring for 12 h to complete the EDC-mediated crosslinking reaction and to simultaneously evaporate the DCM solvent. The obtained mixture was centrifuged (6 000 rpm, 5 min) to get the precipitate, followed by washing 3 times with water. The formed γ-PGA/PEI-Fe_3O_4 NGs were finally redispersed in water before use. For some characterizations, a portion of the NGs were lyophilized to give a black powder. For comparison with the NGs, PEI-Fe_3O_4 NPs were carboxylated by succinic anhydride to fabricate the PEI-Fe_3O_4-SAH NPs with carboxyl groups according to the method reported by Cai *et al*.[13]

Characterization techniques

Dynamic light scattering (DLS) and zeta potential measurements were performed using a Malvern Zetasizer Nano ZS model ZEN3600 (Worcestershire, UK) equipped with a standard 633 nm laser. The PEI-Fe_3O_4 NPs and γ-PGA/PEI-Fe_3O_4 NGs were dispersed in water before measurements. The crystal structure of the γ-PGA/PEI-Fe_3O_4 NGs was identified by X-ray diffraction (XRD) using a D/max 2550 PC X-ray diffractometer (Rigaku Cop., Tokyo, Japan) with Cu Kα radiation (λ= 0.154056 nm) at 40 kV and 200 mA and a 2θ range of 10-80°. Fourier transform infrared (FTIR) spectra of γ-PGA, PEI-Fe_3O_4 NPs, and γ-PGA/PEI-Fe_3O_4 NGs were recorded on a Nicolet Nexus 670 FITR spectrometer (Thermo Nicolet Corporation, Madison, WI). Thermal gravimetric analysis (TGA) was performed on a TG 209 F1 thermogravimetric analyzer (NETZSCH Instruments Co., Ltd., Selb/Bavaria, Germany) from room temperature to 900 °C at a heating rate of 10 °C/min under nitrogen atmosphere. Transmission electron microscopy (TEM) was conducted using a JEOL 2010F analytical electron microscope (Tokyo, Japan) with an accelerating voltage of 200 kV. TEM samples were prepared by depositing a dilute NG suspension (5 μL) onto a carbon-coated copper grid and air-dried before measurements. Field emission scanning electron microscopy (FE-SEM) was operated using a Hitachi scanning electron microscope (Tokyo, Japan) at an operating voltage of 5 kV. Samples were prepared by depositing a dilute NG suspension (5 μL) onto aluminum foil and air-dried before measurements. The Fe concentration of the γ-PGA/PEI-Fe_3O_4 NG suspension was determined by a Leeman Prodigy ICP-OES system (Hudson, NH). T_2 relaxometry of the γ-PGA/PEI-Fe_3O_4 NGs was performed by a NMI20-Analyst NMR Analyzing System (Shanghai Niumag Corporation, Shanghai, China). The NGs were diluted in 2 mL water at different Fe concentrations (0.0125-0.2 mM) before measurements. A CPMG sequence was employed to measure the T_2 relaxation times under the following instrumental parameters: point resolution = 156 mm × 156 mm, section thickness = 0.6 mm, TR = 3500 ms, TE = 90 ms, and

number of excitation = 1. The T_2 relaxivity (r_2) was calculated by linear fitting of $1/T_2$ (s^{-1}) as a function of Fe concentration.

Cytotoxicity assay and cell morphology observation

HeLa cells were cultured and passaged in DMEM supplemented with 10% (*v*/*v*) heat-inactivated FBS, penicillin (100 U/mL), and streptomycin (100 μg/mL) in a humidified incubator containing 5% CO_2 at 37 °C. *In vitro* cytotoxicity of the γ-PGA/PEI-Fe_3O_4 NGs was evaluated by CCK-8 assay. Briefly, HeLa cells were plated in a 96-well plate at a density of 1×10^4 cells per well with 200 μL of DMEM and cultured at 37 °C and 5% CO_2 overnight. Then the medium was replaced by 200 μL fresh medium containing PBS (control) and γ-PGA/PEI-Fe_3O_4 NGs at varying Fe concentrations (0.01, 0.02, 0.04, 0.06, 0.08, 0.1, and 0.2 mM, respectively). After incubation for 24 h, the medium in each well was substituted with 200 μL DMEM containing 20 μL CCK-8. The cells were incubated for another 4 h under regular culture conditions. Finally, the absorbance of each well was measured using a Thermo Scientific Multiskan MK3 ELISA reader (Waltham, MA) at 450 nm. Mean and standard deviation (SD) of 5 parallel wells for each sample were reported.

To further assess the cytotoxicity of the γ-PGA/PEI-Fe_3O_4 NGs, the morphology of HeLa cells treated with the NGs for 24 h was observed by phase contrast microscopy (Leica DM IL LED inverted phase contrast microscope, Wetzlar, Germany) at a magnification of 100 × for each sample.

***In vitro* cellular uptake**

To prove the cellular uptake of the γ-PGA/PEI-Fe_3O_4 NGs, Prussian blue staining assay was performed. Briefly, HeLa cells were seeded in a 6-well plate at a density of 4×10^5 cells per well and incubated with 2 mL DMEM overnight. Subsequently, the medium was replaced by 2 mL fresh DMEM containing PBS (control), PEI-Fe_3O_4-SAH NPs or γ-PGA/PEI-Fe_3O_4 NGs ([Fe] = 0.05 or 0.1 mM, respectively). After incubated for 4 h, the cells were washed 3 times with PBS and fixed by 2.5% glutaraldehyde in PBS at 4 °C for 15 min. Eventually, the cells were washed by PBS and stained by 2 mL Prussian blue reagent (1% potassium ferrocyanide aqueous solution mixed with 2% HCl by equally volume) for 30 min in the dark. The cells were observed by phase contrast microscopy (Leica DM IL LED inverted phase contrast microscope) with a magnification of 100 × for each sample.

To quantify the cellular Fe uptake, HeLa cells were seeded in a 6-well plate at a density of 4×10^5 cells per well with 2 mL DMEM. After incubated overnight, the medium was replaced with fresh medium containing PEI-Fe_3O_4-SAH NPs or γ-PGA/PEI-Fe_3O_4 NGs at different Fe concentrations (0.02, 0.04, 0.08, 0.1, and 0.2 mM, respectively). Thereafter, the cells were incubated for 4 h, washed with PBS for 3 times, trypsinized, resuspended, and counted. Then the cells were lysed using an aqua regia (2 mL, nitric acid/hydrochloric acid, *v*/*v* = 1:3), followed by quantification of Fe with ICP-OES. Data were given as mean ± SD (n = 5).

To further observe the cellular uptake of the γ-PGA/PEI-Fe_3O_4 NGs, TEM imaging of HeLa cells was carried out. HeLa cells were seeded in a 6-well plate at a density of 4×10^5 cells per well and incubated with 2 mL DMEM overnight. The medium was removed and replaced by 2 mL DMEM containing PBS (control) and γ-PGA/PEI-Fe_3O_4 NGs at a Fe concentration of 0.1 mM. After incubated for 4 h, the cells were washed 3 times with PBS and fixed with 2.5% glutaraldehyde in PBS at 4 °C for 1 h. Following a standard protocol reported in the literature,[34] the cells were processed and observed by TEM.

***In vitro* MR imaging of cancer cells**

HeLa cells were seeded in a 6-well plate at a density of 4×10^5 cells per well and incubated with 2 mL DMEM at 37 °C and 5% CO_2 overnight. Then the medium was replaced by 2 mL DMEM containing PBS (control) and γ-PGA/PEI-Fe_3O_4 NGs at varying Fe concentrations (0.025, 0.05, 0.1, and 0.2 mM, respectively). After incubated for 4 h, the cells were washed with PBS for 3 times, trypsinized, centrifuged, and resuspended in 0.5 mL agarose (0.5%) in 2-mL Eppendorf tubes before MR scanning. T_2-weighted MR imaging of the cell suspensions was performed using a 3.0 T SIEMENS MAGNETOM VERIO clinical MR system (SIEMENS Medical Systems, Erlangen, Germany) with the following parameters: slice thickness = 0.9 mm, TR = 7500 ms , TE = 77 ms, FOV = 9 × 9 cm, and matrix = 256 × 256.

***In vivo* MR imaging of a xenografted tumor model**

Animal experiments were carried out according to protocols approved by the institutional committee for animal care, and also in accordance with the policy of the National Ministry of Health. Male 4- to 6-week-old BALB/c nude mice (20-25 g, Shanghai Slac Laboratory Animal Center, Shanghai, China) were used to establish a tumor model using a method described in the literature.[35] Each mouse was injected with HeLa cells (4×10^6 cells in 0.2 mL PBS) into its oxter. After 3-4 weeks injection, when tumor nodule reached 1 cm, the mice were sacrificed, and the fresh tumor tissue was cut into 1 mm blocks, washed with physiological saline for 6 times, grinded into cell suspension, and redispersed in physiological saline. Afterwards, 0.1 mL of the above cell suspension (1×10^6 cells) was subcutaneously injected into the each mouse's hind leg. At two weeks post tumor inoculation, when the tumor size reached about 5 mm, the mice were anesthetized by intraperitoneal injection of pentobarbital sodium (40 mg/kg), and then intravenously injected with the γ-PGA/PEI-Fe_3O_4 NGs *via* the tail vein ([Fe] = 51.04 mM, 0.2 mL PBS, for each mouse). The mice were placed inside a custom-built rodent receiver coil (Chenguang Med Tech, Shanghai, China), and MR scanning was carried out before and after administration of the γ-PGA/PEI-Fe_3O_4 NGs at the time points of 2, 4, and 6 h postinjection. MR scanning was performed using a 3.0 T SIEMENS MAGNETOM VERIO clinical MR system with the same parameters as those used for *in vitro* cell MR imaging.

***In vivo* biodistribution and H&E staining**

The tumor-bearing BALB/c nude mice treated with the γ-PGA/PEI-Fe_3O_4 NGs at different time points postinjection were euthanized and the major organs including the heart, liver, spleen, lung, kidney and tumor were extracted and weighed. The organs were cut into small pieces and digested by aqua regia (2 mL) overnight before ICP-OES quantification of the Fe element. For comparison, the tumor-bearing mice without injection were used as control.

To further elucidate the biodistribution and organ compatibility of the NGs, healthy Kunming mice (30-40 g, Shanghai SLAC Laboratory Animal Center, Shanghai, China) were intravenously injected with the γ-PGA/PEI-Fe_3O_4 NGs ([Fe] = 51.04 mM, 0.2 mL PBS, for each mouse). The mice were euthanized at 7, 14, and 30 days postinjection and the major organs including the heart, liver, spleen, lung, and kidney were extracted, weighed, and digested using aqua regia, followed by quantification of the Fe using ICP-OES. In parallel, the corresponding organs were fixed with 10% neutral buffered formalin, embedded in paraffin, sectioned into slices with a thickness of 4 μm, and stained with hematoxylin and eosin (H&E) using a standard procedure reported in the literature.[36] The organ sections were observed using a Leica DM IL LED inverted phase contrast microscope.

Statistical analysis

One-way ANOVA statistical analysis was performed to evaluate the significance of the experimental data. 0.05 was selected as the significance level, and the data were indicated with (*) for $p < 0.05$, (**) for $p < 0.01$, and (***) for $p < 0.001$, respectively.

Results and discussion

Synthesis and characterization of the γ-PGA/PEI-Fe_3O_4 NGs

Using a double emulsion method and the synthesized PEI-Fe_3O_4 NPs as a crosslinker, γ-PGA/PEI-Fe_3O_4 NGs were able to be prepared (Scheme 1). The formed NGs were then characterized *via* different techniques. DLS and zeta potential measurements were used to characterize the hydrodynamic size and surface potential of the formed PEI-Fe_3O_4 NPs, PEI-Fe_3O_4-SAH NPs and γ-PGA/PEI-Fe_3O_4 NGs in aqueous solution (Table 1). The PEI-coated Fe_3O_4 NPs display a hydrodynamic size of 132.4 ± 1.21 nm with a positive surface potential of 41.7 ± 0.66 mV, corroborating the literature data.[14] The PEI-Fe_3O_4-SAH NPs display a slightly larger hydrodynamic size of 148.9 ± 4.80 nm with a negative surface potential of -23.1 ± 0.53 mV. After the formation of the γ-PGA/PEI-Fe_3O_4 NGs, the NGs show an increased hydrodynamic size of 239.4 ± 3.80 nm (Fig. S1a, Electronic Supplementary Information, ESI) with an inversed surface potential of -6.55 ± 0.66 mV. These results are in line with the initial molar feeding ratio of PEI amine/γ-PGA carboxyl at 1:10. It is interesting to note that the used initial molar feeding ratio of PEI amine/γ-PGA carboxyl at 1:10 is optimal, NGs prepared using other ratios at 1:1, 1:2, 1:4, 1:6, or 1:8 do not seem to be sufficiently stable. The γ-PGA/PEI-Fe_3O_4 NGs display a good colloidal stability, and their hydrodynamic size does not appreciably change after being stored for a period of 15 days (Fig. S1b). To further explore the stability of the NGs in an intracellular environment, the hydrodynamic size of the NGs both in an acidic aqueous solution (pH = 6.5) and in an acidic aqueous solution (pH = 6.5) containing high GSH concentrations (10 or 30 μM) was measured at different time points (Fig. S2, ESI). It can be seen that the acidic environment does not impact the stability of the NGs, while the presence of GSH slightly increases the size of the NGs, possibly due to the physical adsorption of the GSH on the surface of the NGs. This further confirmed the good colloidal stability of the NGs, which is essential for their MR imaging applications.

To verify the existence of Fe_3O_4 NPs within the NGs, the crystalline structure of the formed γ-PGA/PEI-Fe_3O_4 NGs was characterized by XRD (Fig. S3, ESI). Clearly, the lattice spacing at 2θ of 30.2, 35.4, 43.5, 53.4, 57.1, and 62.7° well matches the [220], [311], [400], [422], [511], and [440] planes of Fe_3O_4 crystals, respectively, in consistence with the literature.[13, 14] This suggests the successful incorporation of Fe_3O_4 NPs within the NGs. FTIR spectroscopy was used to further characterize the structure of the formed PEI-Fe_3O_4-SAH NPs and hybrid NGs (Fig. 1). It can be seen that the appearance of the typical absorption peak at 598 cm^{-1} for PEI-Fe_3O_4 NPs (Fig. 1, curve b), PEI-Fe_3O_4-SAH NPs (Fig. 1, curve c) and the γ-PGA/PEI-Fe_3O_4 NGs (Fig. 1, curve d) can be assigned to the Fe-O bond. The emerging peak around 1420 cm^{-1} in cruve c could be caused by the stretching vibration of N-C bond of the formed succinamic acid ($NHCOCH_2CH_2COOH$), indicating the success of the tranformation of PEI amines to PEI succinamic acids. The peaks at around 2925 cm^{-1} and 1377 cm^{-1} in curve d could be due to the vibrations of -CH_2- symmetric stretching and -NH_2 scissoring, respectively. And the new peak at 1737 cm^{-1} in curve d should be attributed to the vibration of amide bond, confirming the successful crosslinking reaction.

Both TEM (Fig. 2a) and FE-SEM (Fig. 2b) were used to observe the morphology of the formed γ-PGA/PEI-Fe_3O_4 NGs. It can be seen that the cluster structure of the PEI-Fe_3O_4 NPs can be formed after the formation of hybrid NGs and the size of each NG can be estimated to be 152.3 ± 13.1 nm. Interestingly, the measured hydrodynamic size of the NGs is much larger than that observed by TEM and FE-SEM. This is likely attributed to the fact that DLS measures the size of aggregated NGs in aqueous solution while TEM and FE-SEM measure single NGs in a dry state.

The loading of Fe_3O_4 NPs within the hybrid NGs were quantified by TGA (Fig. S4, ESI). Obviously, by comparison of the weight percentage of the naked Fe_3O_4 and the PEI-Fe_3O_4 NPs at 850 ^oC, the PEI coating onto the surface of the Fe_3O_4 NPs can be estimated to be 15.1%, approximately similar to the literature data.[14] Similarly, by subtraction of the weight loss of the PEI-Fe_3O_4 NPs from that of the hybrid NGs, the content of γ-PGA can be estimated to be 45.2%. In this context, the loading of Fe_3O_4 NPs can be estimated to be 54.8%.

T_2 relaxometry

The existence of Fe_3O_4 NPs enables the NGs to be potentially used as a contrast agent for T_2-weighted MR imaging applications. We tested the T_2 relaxometry of the hybrid NGs (Fig. 3). It can be seen that with the increase of Fe concentration, the MR signal intensity of the NGs gradually decreases (Fig. 3a). By plotting the relaxation rate ($1/T_2$) as a function Fe concentration (Fig. 3b), the r_2 relaxivity of the NGs was computed to be 171.1 $mM^{-1}s^{-1}$. Compared to the r_2 relaxivity (545.70 $mM^{-1}s^{-1}$) of the individual PEI-Fe_3O_4 NPs synthesized by the mild reduction method,[14] the r_2 value of the hybrid NGs is quite low. This is likely due to the possible aggregation of the PEI-Fe_3O_4 NPs within the NGs and also the barrier effect of the γ-PGA NGs, quite restricting the accessibility of water protons to the surface of Fe_3O_4 NPs. In any case, the γ-PGA/PEI-Fe_3O_4 NGs still display a larger r_2 relaxivity than the commercial Feridex® and Resovist® product[37] and also other individual functionalized Fe_3O_4 NPs synthesized using other approaches,[3, 4, 6, 10, 12, 13

ensuring their uses as a promising contrast agent for MR imaging applications.

Cytotoxicity assay and cell morphology observation

Before biomedical applications, it is essential to test the cytocompatibility of the hybrid NGs. CCK-8 assay was executed to evaluate the cytotoxicity of the γ-PGA/PEI-Fe_3O_4 NGs (Fig. 4). Obviously, the viability of HeLa cells is higher than 100% after incubation with NGs in the given Fe concentration range (0.01-0.2 mM), suggesting their excellent cytocompatibility. As reported in the literature,[28, 38] γ-PGA can be considered as one nutritional factor that promotes the cell growth, migration, and proliferation, similar to the cytotoxicity data of γ-PGA-coated $MnFe_2O_4$ NPs.[39]

In order to visually confirm the cytocompatibility of the hybrid NGs, HeLa cells treated with the NGs at different Fe concentrations were observed by phase contrast microscope (Fig. S5, ESI). It can be seen that HeLa cells treated with the hybrid NGs in Fe concentration range of 0.01-0.2 mM do not display any appreciable morphological changes when compared with the control cells treated with PBS. The cell morphology observation corroborates the CCK-8 assay data, suggesting that the γ-PGA/PEI-Fe_3O_4 NGs are non-cytotoxic in the given Fe concentration range.

***In vitro* cellular uptake of the hybrid NGs**

For MR imaging of cancer cells *in vitro* and tumors *in vivo*, it is important to check if the developed hybrid NGs can be endocytosed. Prussian blue staining is first carried out to check the ability of the NGs to be uptaken by cancer cells after treatment for 4 h (Fig. 5). There are scarcely blue stains in the control cells treated with PBS, while the HeLa cells treated with the NGs display apparent blue stains, which are associated to the Fe_3O_4 NP-containing NGs uptaken by the cells. The cellular uptake of the NGs was also compared with the single PEI-Fe_3O_4-SAH NPs. Clearly, under the same Fe concentration, the cells treated with NGs show a much darker blue staining than those treated with the NPs, indicating that the NGs enable an enhanced Fe uptake in cells, possibly due to the softness of the NGs.[18] In addition, the blue staining of cells is more prominent with the increase of Fe concentration for both NPs and NGs. The cellular uptake of both NGs and NPs may occur through two distinct mechanisms: phagocytosis and diffusion *via* cell walls, in agreement with the literature.[16, 40]

The cellular uptake of the single PEI-Fe_3O_4-SAH NPs and hybrid NGs was further quantitatively confirmed by ICP-OES (Fig. 6). It can be seen that the cellular Fe uptake of NGs is much higher than that of the NPs under a given Fe concentration ($p < 0.01$). For both the NPs and NGs, the cellular Fe uptake gradually increases with the increase of the Fe concentration. At the highest Fe concentration tested (0.2 mM), the cells can uptake 10.37 pg Fe/cell of NGs (4 times of the NPs), confirming that the hybrid NGs displays a much more enhanced cellular uptake than the NPs, which is beneficial for further sensitive MR imaging applications.

To further investigate the detailed uptake of the γ-PGA/PEI-Fe_3O_4 NGs at cellular compartments, TEM imaging of HeLa cells was performed (Fig. 7). We can see that HeLa cells treated with the NGs for 4 h display an apparent staining predominantly in the vacuoles of the cells (Fig. 7b). In contrast, control cells treated with PBS do not display such staining (Fig. 7a). This further confirmed the ability of the hybrid NGs to be endocytosed by cancer cells, regardless their relatively large size (152.3 ± 13.1 nm). It should be noted that due to the softness and excellent fluidity of the NGs, the NGs once uptaken by the intracellular compartment display irregular shape, which is different from those measured by TEM and SEM. In certain cases, aggregated NGs are located in a particular intracellular compartment.

***In vitro* MR imaging of cancer cells**

With the proven cytocompatibility and the ability to be endocytosed, we next explored the potential to use the developed hybrid NGs as a contrast agent for MR imaging of cancer cells *in vitro*. T_2-weighted MR images of HeLa cells treated with the γ-PGA/PEI-Fe_3O_4 NGs at different Fe concentrations were obtained and the signal to noise ratio (SNR) of the cells was quantified (Fig. 8). It is clear that the hybrid NGs are able to decrease the MR signal intensity of the cells with the increase of Fe concentration (Fig. 8a). This can be further clearly reflected by quantitative analysis of the MR SNR of the cells as a function of Fe concentration (Fig. 8b). Apparently, the SNR of the HeLa cells gradually decreases with the Fe concentration, and the MR SNR of HeLa cells at an Fe concentration of 0.2 mM reaches 8.4, about 1/10 of that of the control cells treated with PBS. These results suggest that the developed γ-PGA/PEI-Fe_3O_4 NGs can be used as a promising contrast agent for MR imaging of HeLa cells *in vitro*.

***In vivo* MR imaging of a xenografted tumor model**

We next investigated the feasibility to use the developed γ-PGA/PEI-Fe_3O_4 NGs as a contrast agent for T_2-weighted MR imaging of a xenografted tumor model *in vivo*. After intravenous injection of the NGs (0.2 mL PBS, [Fe] = 51.04 mM) *via* the tail vein, pseudo-colored MR images were collected at different time points (Fig. 9a). Obviously, the MR signal intensity of the tumor region shows a gradual decrease as a function of time postinjection, and at 4 h postinjection the MR signal intensity is the weakest. Then the MR signal intensity of the tumor region starts to recover at 6 h postinjection. Further quantitative evaluation of the MR SNR of tumors reveals the same trend (Fig. 9b). In addition to the tumor region, the liver and kidney display the same trend of MR SNR change. Our results suggest that the γ-PGA/PEI-Fe_3O_4 NGs are able to be delivered to tumor region possibly *via* the passive enhanced permeability and retention (EPR) effect, enabling effective tumor MR imaging. Similarly, a significant portion of the NGs can be recognized by the reticuloendothelial system (RES) located in the liver region and metabolized *via* kidney, therefore, the NGs can also be simultaneously used for MR imaging of mouse liver and kidney.

***In vivo* biodistribution and toxicity evaluations**

It is crucial to figure out the biodistribution behavior of the developed γ-PGA/PEI-Fe_3O_4 NGs for further *in vivo* biomedical imaging applications. ICP-OES was performed to quantitatively analyze the accumulation of Fe in different organs including the heart, liver, spleen, lung, kidney, and tumor at 2, 4, 6, 12, and 24 h post-intravenous injection (Fig. S6a, ESI). It is clear that the Fe concentration in the liver, spleen, and lung of the mice treated with the NGs is much higher than that of the control group. At 4

h postinjection, the tumor has the maximum Fe uptake. Overall, the Fe uptake in the major organs starts to decrease at 6 h postinjection, corroborating the MR imaging data.

To further demonstrate the biocompatibility of the hybrid NGs *in vivo*, healthy mice were intravenously injected with the γ-PGA/PEI-Fe_3O_4 NGs and subjected to biodistribution studies at different time points (Fig. S6b). It is obvious that the Fe concentrations in the major organs of heart, liver, spleen, lung and kidney at 7, 14, 30 days postinjection show no significant difference when compared with the control mice without treatment. This implies that the injected hybrid NGs are able to be completely metabolized and excreted from the body after 7 days, and the NGs do not exert any possible toxicity to the animals. The biocompatibility of the NGs was further confirmed by histological examination of the major organs. H&E staining results (Fig. 10) verify that the thin sections of mouse heart, liver, spleen, lung, and kidney injected with the NGs do not display appreciable morphological changes when compared to the control mice without treatment. Taken together with the biodistribution data, our results suggest that the developed hybrid NGs are pretty biocompatible *in vivo*.

Conclusion

In summary, we developed a facile double emulsion approach to forming Fe_3O_4 NP-loaded γ-PGA NGs for T_2-weighted MR imaging of tumors. Through the EDC-mediated crosslinking reaction between the γ-PGA carboxyl groups and the amines of the PEI-Fe_3O_4 NPs, hybrid NGs with a size of 152.3 ± 13.1 nm can be formed. The developed hybrid NGs are water-dispersible, colloidally stable, cytocompatible in a given Fe concentration range. With the relatively high r_2 relaxivity and the superior ability to be uptaken by cancer cells, the formed γ-PGA/PEI-Fe_3O_4 NGs are able to be used as a promising contrast agent for MR imaging of cancer cells *in vitro* and the xenografted tumor model *in vivo via* the passive EPR effect. The developed hybrid γ-PGA/PEI-Fe_3O_4 NGs may hold great promise to be used as a novel contrast agent for MR imaging or other theranostic applications.

Acknowledgements

This research is financially supported by the Sino-German Center for Research Promotion (GZ899), the National Natural Science Foundation of China (21273032 and 81401458), and the Program for Professor of Special Appointment (Eastern Scholar) at Shanghai Institutions of Higher Learning. C. P. thanks the financial support from the Shanghai Natural Science Foundation (14ZR1432400).

Notes and references

[a] *College of Chemistry, Chemical Engineering and Biotechnology, Donghua University, Shanghai 201620, People's Republic of China*
E-mail: xshi@dhu.edu.cn
[b] *Department of Radiology, Shanghai Tenth People's Hospital, School of Medicine, Tongji University, Shanghai 200072, People's Republic of China*
[c] *State Key Laboratory for Modification of Chemical Fibers and Polymer Materials, College of Materials Science and Engineering, Donghua University, Shanghai 201620, People's Republic of China*
[1] *Jianzhi Zhu and Chen Peng contributed equally to this work.*

† **Electronic supplementary information (ESI) available**: additional experimental results.

1. R. R. Qiao, C. H. Yang and M. Y. Gao, *J. Mater. Chem.*, 2009, **19**, 6274-6293.
2. J. Zeng, L. Jing, Y. Hou, M. Jiao, R. Qiao, Q. Jia, C. Liu, F. Fang, H. Lei and M. Gao, *Adv. Mater.*, 2014, **26**, 2694-2698.
3. X. Y. Shi, S. H. Wang, S. D. Swanson, S. Ge, Z. Y. Cao, M. E. Van Antwerp, K. J. Landmark and J. R. Baker, *Adv. Mater.*, 2008, **20**, 1671-1678.
4. J. C. Li, Y. He, W. J. Sun, Y. Luo, H. D. Cai, Y. Q. Pan, S. M. W.;, J. D. Xia and X. Y. Shi, *Biomaterials*, 2014, **35**, 3666-3677.
5. E. S. G. Choo, X. S. Tang, Y. Sheng, B. Shuter and J. M. Xue, *J. Mater. Chem.*, 2011, **21**, 2310-2319.
6. J. C. Li, L. F. Zheng, H. D. Cai, W. J. Sun, M. W. Shen, G. X. Zhang and X. Y. Shi, *Biomaterials*, 2013, **34**, 8382-8392.
7. X. Y. Shi, T. P. Thomas, L. A. Myc, A. Kotlyar and J. R. Baker, *Phys. Chem. Chem. Phys.*, 2007, **9**, 5712-5720.
8. K. An, M. Park, J. H. Yu, H. B. Na, N. Lee, J. Park, S. H. Choi, I. C. Song, W. K. Moon and T. Hyeon, *Eur. J. Inorg. Chem.*, 2012, **2012**, 2148-2155.
9. C. K. Lim, A. Singh, J. Heo, D. Kim, K. E. Lee, H. Jeon, J. Koh, I. C. Kwon and S. Kim, *Biomaterials*, 2013, **34**, 6846-6852.
10. J. C. Li, X. Y. Shi and M. W. Shen, *Part. Part. Syst. Charact.*, 2014, **31**, 1223-1237.
11. J. Xie, K. Chen, H. Y. Lee, C. Xu, A. R. Hsu, S. Peng, X. Chen and S. Sun, *J. Am. Chem. Soc.*, 2008, **130**, 7542-7543.
12. S. H. Wang, X. Shi, M. Van Antwerp, Z. Cao, S. D. Swanson, X. Bi and J. R. Baker, *Adv. Funct. Mater.*, 2007, **17**, 3043-3050.
13. H. D. Cai, X. An, J. Cui, J. C. Li, S. H. Wen, K. G. Li, M. W. Shen, L. F. Zheng, G. X. Zhang and X. Y. Shi, *ACS Appl. Mater. Interfaces*, 2013, **5**, 1722-1731.
14. Y. Hu, J. C. Li, J. Yang, P. Wei, Y. Luo, L. Ding, W. J. Sun, G. X. Zhang, X. Y. Shi and M. W. Shen, *Biomater. Sci.*, 2015, **3**, 721-732.
15. J. Li, Y. Hu, J. Yang, W. Sun, H. Cai, P. Wei, Y. Sun, G. Zhang, X. Shi and M. Shen, *J. Mater. Chem. B*, 2015, **3**, 5720-5730.
16. H. Ai, C. Flask, B. Weinberg, X. T. Shuai, M. D. Pagel, D. Farrell, J. Duerk and J. M. Gao, *Adv. Mater.*, 2005, **17**, 1949-1951.
17. J. Lu, S. Ma, J. Sun, C. Xia, C. Liu, Z. Wang, X. Zhao, F. Gao, Q. Gong , B. Song, X. Shuai, H. Ai and Z. Gu, *Biomaterials*, 2009, **30**, 2919-2928.
18. Y. Li, D. Maciel, J. Rodrigues, X. Shi and H. Tomás, *Chem. Rev.*, 2015, DOI: 10.1021/cr500131f.
19. A. Pich, A. Tessier, V. Boyko, Y. Lu and H. J. P. Adler, *Macromolecules*, 2006, **39**, 7701-7707.
20. M. Oishi and Y. Nagasaki, *Nanomedicine*, 2010, **5**, 451-468.
21. W. T. Wu and S. Q. Zhou, *Nano Rev.*, 2010, **1**.
22. M. W. Shen, H. D. Cai, X. F. Wang, X. Y. Cao, K. G. Li, S. H. Wang, R. Guo, L. F. Zheng, G. X. Zhang and X. Y. Shi, *Nanotechnology*, 2012, **23**.
23. W. H. Chiang, V. T. Ho, H. H. Chen, W. C. Huang, Y. F. Huang, S. C. Lin, C. S. Chern and H. C. Chiu, *Langmuir*, 2013, **29**, 6434-6443.
24. L. Y. Jiang, Q. Zhou, K. T. Mu, H. Xie, Y. H. Zhu, W. Z. Zhu, Y. B. Zhao, H. B. Xu and X. L. Yang, *Biomaterials*, 2013, **34**, 7418-7428.
25. S. Singh, M. Moller and A. Pich, *J. Polym. Sci., Part A: Polym. Chem.*, 2013, **51**, 3044-3057.
26. T. Nochi, Y. Yuki, H. Takahashi, S. Sawada, M. Mejima, T. Kohda, N. Harada, I. G. Kong, A. Sato, N. Kataoka, D. Tokuhara, S. Kurokawa, Y. Takahashi, H. Tsukada, S. Kozaki, K. Akiyoshi and H. Kiyono, *Nat. Mater.*, 2010, **9**, 572-578.
27. T. W. Kim, T. Y. Lee, F. C. Bae, J. H. Hahm, Y. H. Kim, C. Park, T. H. Kang, C. J. Kim, M. H. Sung and H. Poo, *J. Immunol.*, 2007, **179**, 775-780.
28. S. R. Bae, C. Park, J. C. Choi, H. Poo, C. J. Kim and M. H. Sung, *J. Microbiol. Biotechnol.*, 2010, **20**, 803-808.
29. B. J. Park, B. J. Kwon, J. K. Kang, M. H. Lee, I. Han, J. K. Kim and J. C. Park, *Macromol. Res.*, 2011, **19**, 537-541.
30. S. G. Wang, J. Y. Zhu, M. W. Shen, M. F. Zhu and X. Y. Shi, *ACS Appl. Mater. Interfaces*, 2014, **6**, 2153-2161.

31. S. Wang, X. Cao, M. Shen, R. Guo, I. Bányai and X. Shi, *Colloids Surf., B*, 2012, **89**, 254-264.
32. D. Maciel, P. Figueira, S. L. Xiao, D. M. Hu, X. Y. Shi, J. Rodrigues, H. Tomas and Y. L. Li, *Biomacromolecules*, 2013, **14**, 3140-3146.
33. M. Goncalves, D. Maciel, D. Capelo, S. L. Xiao, W. j. Sun, X. Y. Shi, J. Rodrigues, H. Tomas and Y. L. Li, *Biomacromolecules*, 2014, **15**, 492-499.
34. H. Wang, L. Zheng, C. Peng, M. Shen, X. Shi and G. Zhang, *Biomaterials*, 2013, **34**, 470-480.
35. H. D. Soule and C. M. McGrath, *In Vitro Cell. Dev. Biol.*, 1986, **22**, 6-12.
36. C. Peng, J. B. Qin, B. Q. Zhou, Q. Chen, M. W. Shen, M. F. Zhu, X. W. Lu and X. Y. Shi, *Polym. Chem.*, 2013, **4**, 4412-4424.
37. M. Molina, M. Asadian-Birjand, J. Balach, J. Bergueiro, E. Miceli and M. Calderon, *Chem. Soc. Rev.*, 2015, **44**, 6161-6186.
38. Z. Q. Xu, P. Lei, X. H. Feng, X. J. Xu, F. H. Liang, B. Chi and H. Xu, *Plant Physiol. Biochem.*, 2014, **80**, 144-152.
39. H. M. Kim, H. Lee, K. S. Hong, M. Y. Cho, M. H. Sung, H. Poo and Y. T. Lim, *ACS Nano*, 2011, **5**, 8230-8240.
40. H. Wang, L. Zheng, C. Peng, R. Guo, M. Shen, X. Shi and G. Zhang, *Biomaterials*, 2011, **32**, 2979-2988.

Table 1. Zeta potentials and hydrodynamic sizes of the PEI-Fe_3O_4 NPs, PEI-Fe_3O_4-SAH NPs, and γ-PGA/PEI-Fe_3O_4 NGs. Data are provided as mean ± SD (n = 3).

Materials	Zeta potential (mV)	Hydrodynamic size (nm)	Polydispersity index (PDI)
PEI-Fe_3O_4 NPs	41.7 ± 0.66	132.4 ± 1.21	0.16 ± 0.01
PEI-Fe_3O_4-SAH NPs	-23.1 ± 0.53	148.9 ± 4.80	0.24 ± 0.04
γ-PGA/PEI-Fe_3O_4 NGs	-6.55 ± 0.42	239.4 ± 3.80	0.13 ± 0.03

Figure captions

Scheme 1. Schematic illustration of the preparation of γ-PGA/ PEI-Fe_3O_4 NGs.

Fig. 1. FTIR spectra of γ-PGA (a), PEI-Fe_3O_4 NPs (b), PEI-Fe_3O_4-SAH NPs (c), and γ-PGA/PEI-Fe_3O_4 NGs (d).

Fig. 2. TEM (a) and FE-SEM (b) images of the γ-PGA/PEI-Fe_3O_4 NGs.

Fig. 3. (a) T_2-weighted MR images of the γ-PGA/PEI-Fe_3O_4 NGs in aqueous solution at Fe concentrations of 0.025, 0.05, 0.1 and 0.2 mM, respectively. The color bar (from red to blue) indicates the gradual decrease of MR signal intensity; (b) T_2 relaxation rate ($1/T_2$) of γ-PGA/PEI-Fe_3O_4 NGs as a function of Fe concentration.

Fig. 4. CCK-8 assay of HeLa cells treated with the γ-PGA/PEI-Fe_3O_4 NGs at varying Fe concentrations (0.01, 0.02, 0.04, 0.06, 0.08, 0.1, and 0.2 mM, respectively) for 24 h.

Fig. 5. Prussian blue staining of HeLa cells treated with the PEI-Fe_3O_4-SAH NPs and γ-PGA/PEI-Fe_3O_4 NGs at Fe concentration of 0.05 mM and 0.1 mM for 4 h.

Fig. 6. Uptake of Fe in HeLa cells treated with the PEI-Fe_3O_4-SAH NPs and γ-PGA/PEI-Fe_3O_4 NGs at different Fe concentrations (0.02, 0.04, 0.08, 0.1, and 0.2 mM, respectively) for 4 h. HeLa cells treated with PBS were used as control.

Fig. 7. TEM images of HeLa cells treated with PBS (a) and the γ-PGA/PEI-Fe_3O_4 NGs (b) at a Fe concentration of 0.1 mM for 4 h.

Fig. 8. T_2-weighted MR images (a) and MR signal to noise ratio (SNR) analysis (b) of HeLa cells treated with the γ-PGA/PEI-Fe_3O_4 NGs at the Fe concentrations of 0, 0.025, 0.05, 0.1 and 0.2 mM for 4 h. The color bar in (a) from red to blue indicates the gradual decrease of MR signal intensity.

Fig. 9. *In vivo* T_2-weighted MR images (a) and MR signal to noise ratio (SNR) (b) of the nude mice

bearing xenografted HeLa tumors at different time points postinjection of the γ-PGA/PEI-Fe_3O_4 NGs ([Fe] = 51.04 mM, 0.2 mL PBS, for each mouse).

Fig. 10. H&E staining of the sections of the heart, liver, spleen, lung, and kidney in healthy mice at 7 d, 14 d, and 30 d posinjection of the γ-PGA/PEI-Fe_3O_4 NGs ([Fe] = 51.04 mM, 0.2 mL PBS, for each mouse). Organs from untreated mice were used as control.

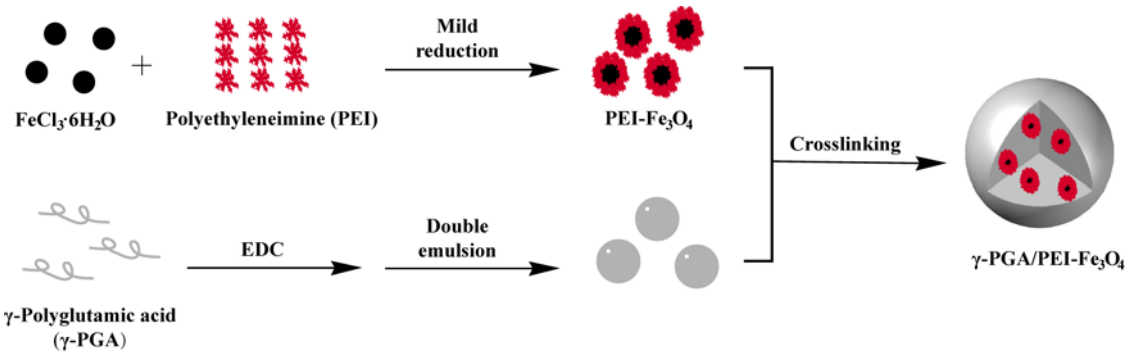

Scheme 1

Zhu *et al.*

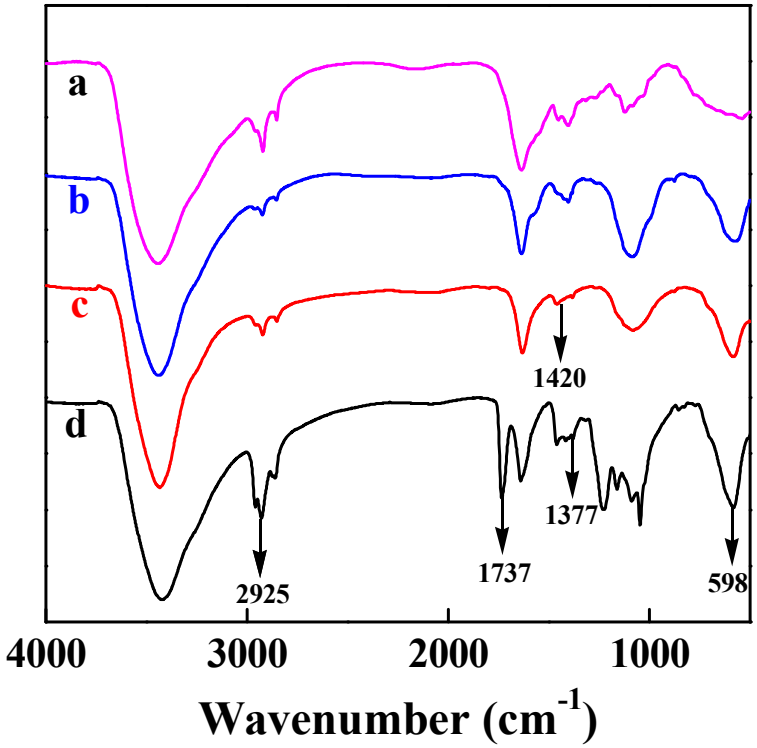

Fig. 1

Zhu *et al.*

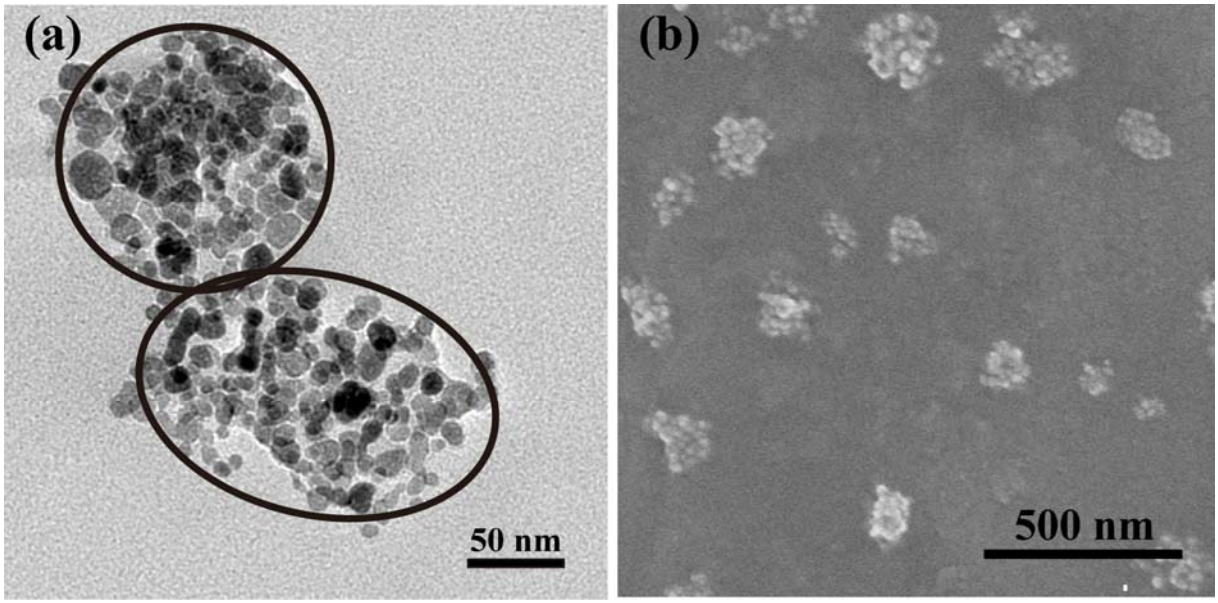

Fig. 2

Zhu *et al*.

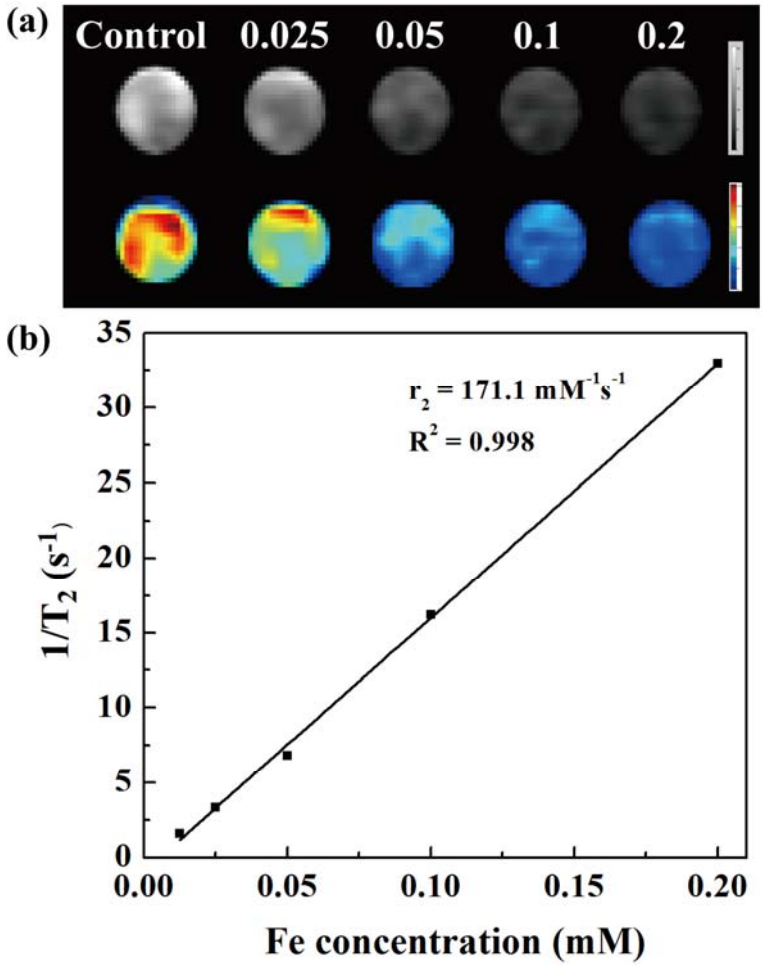

Fig. 3

Zhu *et al.*

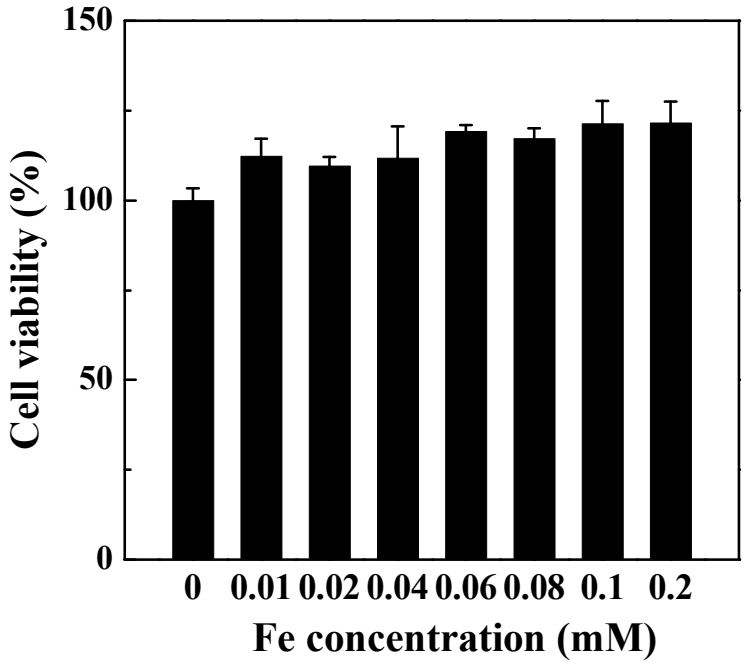

Fig. 4

Zhu *et al*.

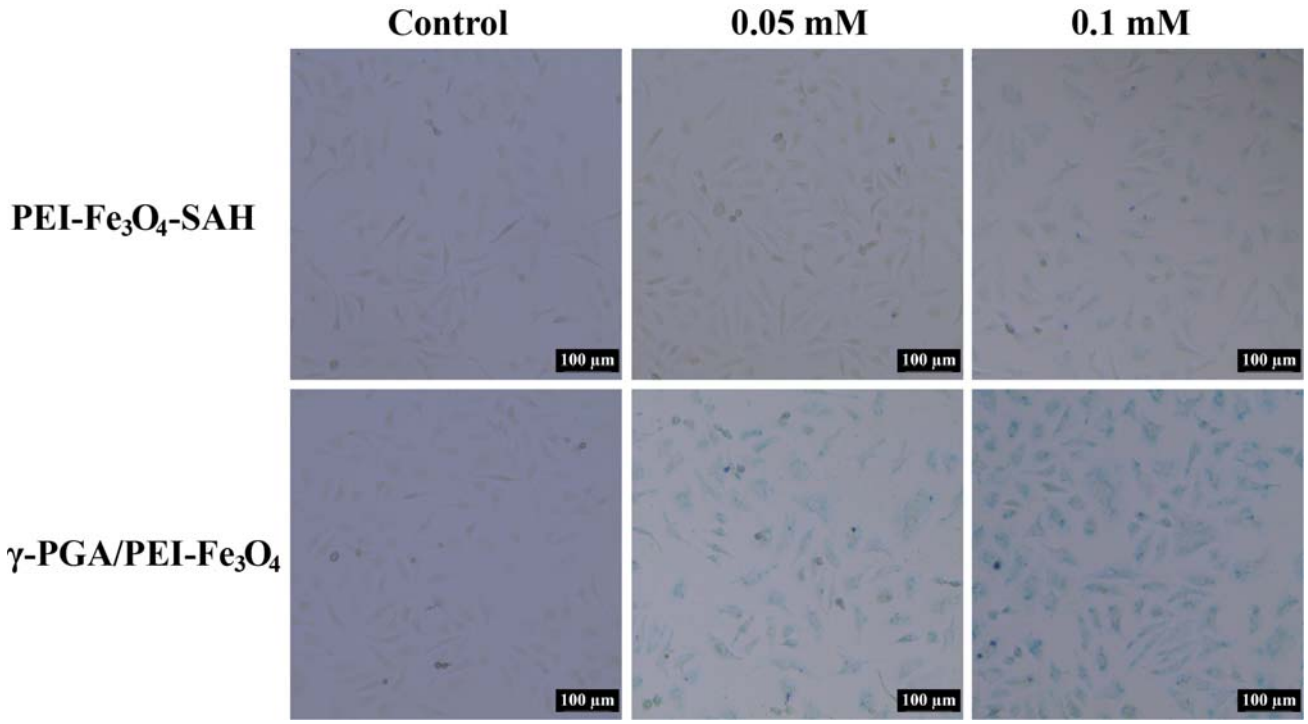

Fig. 5

Zhu *et al*.

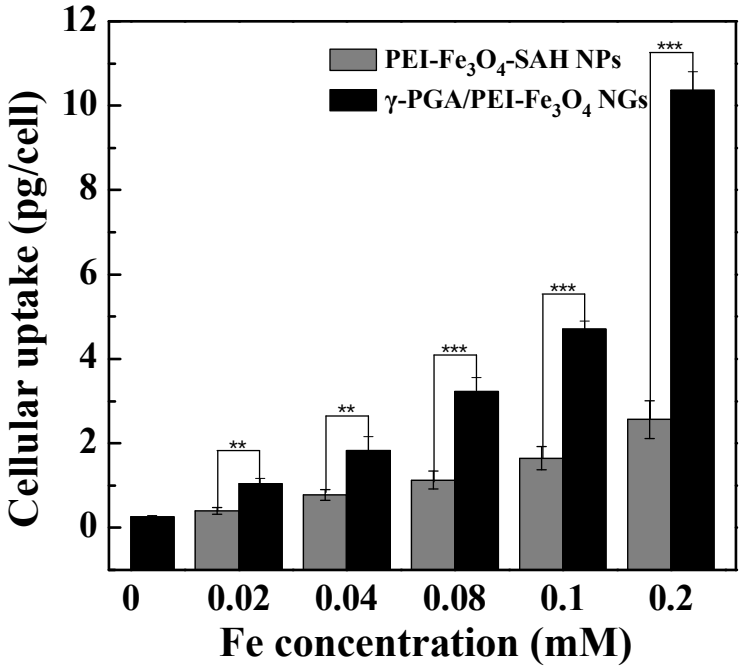

Fig. 6

Zhu *et al.*

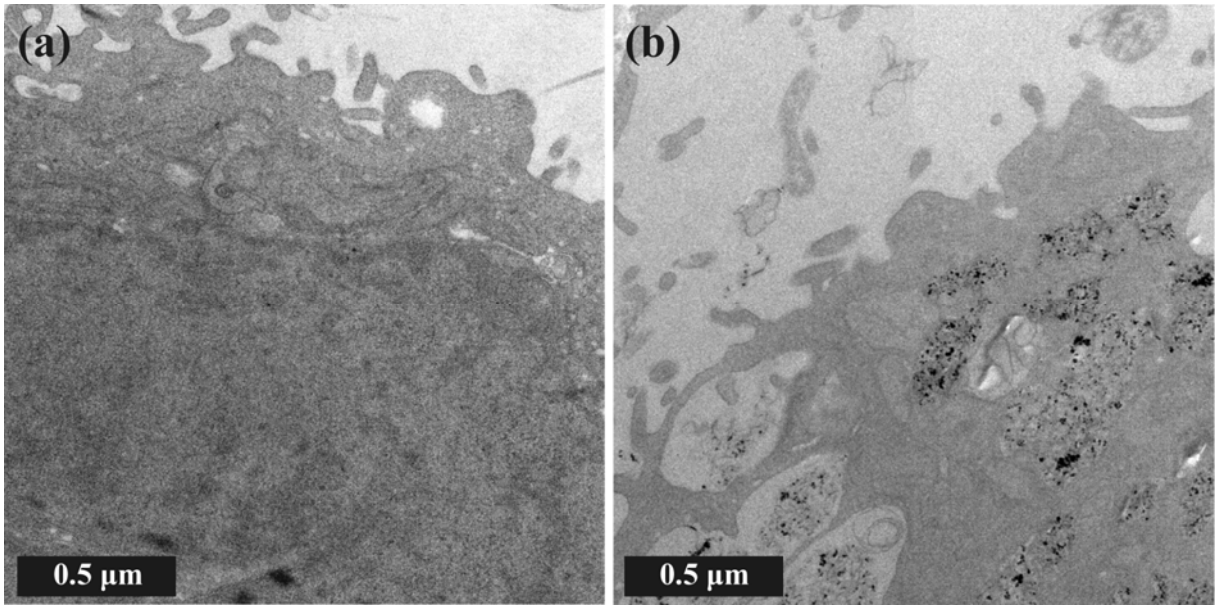

Fig. 7

Zhu *et al*.

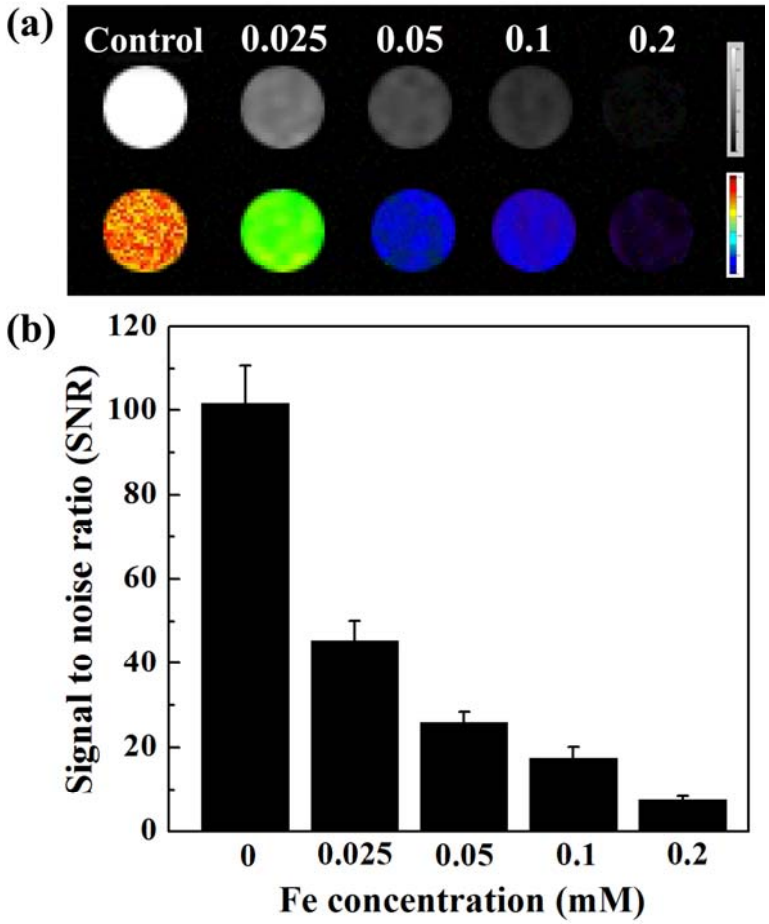

Fig. 8

Zhu *et al.*

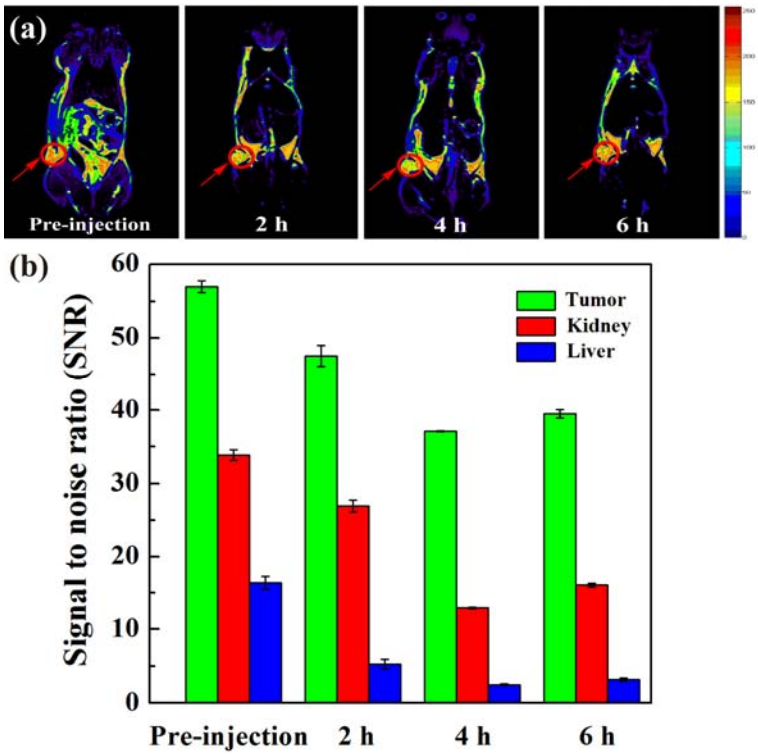

Fig. 9

Zhu *et al.*

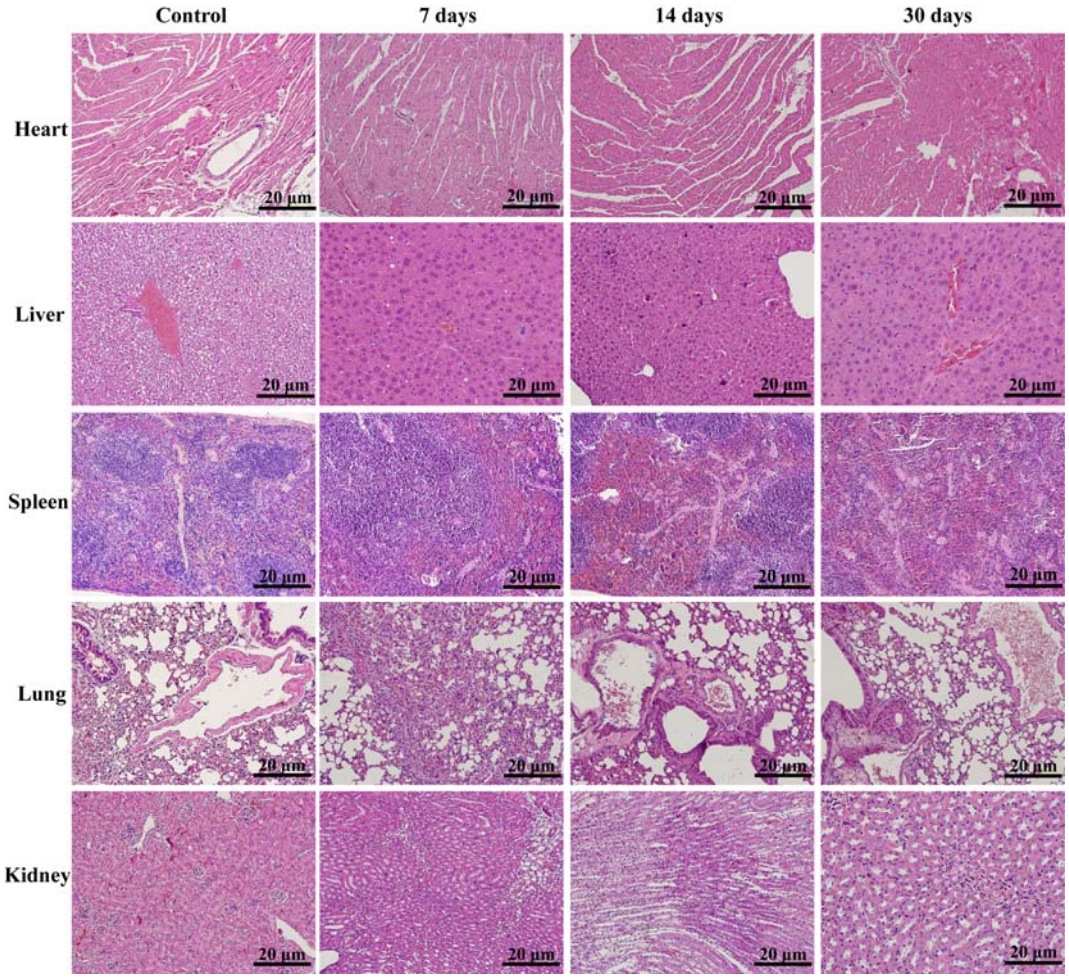

Fig. 10

Zhu *et al.*

Table of Contents (TOC)

Formation of iron oxide nanoparticle-loaded γ-polyglutamic acid nanogels for MR imaging of tumors†

Jianzhi Zhu,[a1] Chen Peng,[b1] Wenjie Sun,[a] Zhibo Yu,[c] Benqing Zhou,[a] Du Li,[c] Yu Luo,[a] Ling Ding,[a] Mingwu Shen,[a] and Xiangyang Shi[a,c]*

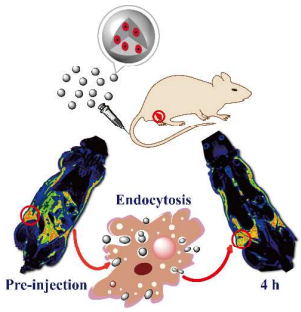

Iron oxide nanoparticle-loaded γ-polyglutamic acid nanogels can be formed through a facile double emulsion approach for MR imaging of tumors.